Journal of Hydroscience and Hydraulic Engineering
Vol. 10, No. 2, November, 1992, 61-79

RESPONSE OF INTERNAL SEICHE TO WIND IN A TWO-LAYERED STRATIFIED LAKE

By

Katsuhiro Furumoto

Dept. of Civil Engineering, Nagasaki University,
Nagasaki 852, Japan

Takehiro Takemasa

Cooperative Research Center, Nagasaki University,
Nagasaki 852, Japan

and

Hiroaki Komoda

Graduate School of Marine Science and Engineering, Nagasaki University,
Nagasaki 852, Japan

SYNOPSIS

The dynamic response of a two-layered stratified lake subject to the wind stress was investigated theoretically and experimentally. The fundamental equations for the currents in the upper and lower layers, as well as the elevations of the water surface and its interface were solved to determine the dynamic response of the lake to the instantaneous rise in the wind stress over the water surface. The solutions were applied to simulate the vertical oscillations of the interface in response to a succession of wind pulses representing the actual wind conditions. The oscillations obtained from theory in comparison with those from experiments and field observations show a good agreement.

INTRODUCTION

The vertical structure of water temperature in a lake and storage reservoir is controlled by the heat transfer from the water surface, turbulent mixing due to wind, temperature and volume of the inflowing water, etc. Usually, a remarkable thermocline layer is formed from summer to the beginning of fall.

Moreover, the density stratification of salinity and other materials is formed in the freshening process of the artificial lake created by closing the inner side of the estuary.

When the wind acts on a closed basin of a two-layered stratified field, the internal seiche and interfacial wave occur on the interface of the discontinuous density in the same manner as the ordinary seiche and wind wave on the free surface of a homogeneous closed basin.

A number of theoretical and experimental researches (10),(17) have been done on a small-scaled interfacial wave of discontinuous stratified layer generated by wind. This is because it deepens the understanding of a discontinuous stratified layer and the entrainment phenomena generating the mass transportation from non-turbulent layer to turbulent layer.

On the other hand, attention for large-scale internal wave in stratified density field has been paid in the field of oceanography in an early period of time due to the accumulation of observation data (3) and the advancement of the theoretical research (16). In Japan, some researches on internal seiche had been done in Lake Biwa (7),(8) and Lake Chuzenji (11),(12) etc. These researches were performed to investigate, only from qualitative point of view, the response properties of the stratified field to the external force of wind, and the

oscillatory characteristics of internal seiche following the stopping of wind. In these researches it was confirmed that the observed period of internal seiche agrees almost with the results of eigenvalue analysis for the condition of density stratification. However, the interfacial displacement and the current responding to wind stress are not yet investigated quantitatively.

On the other hand, a theoretical study on internal seiche by Heaps and Ramsbottom (4) was performed. Nevertheless, in their study the experiments and the observations to examine the validity are lack. Therefore the basic problem concerning with the damping of wave height is left over. In this paper, the authors executed the field observation in Ohno Reservoir of Tottori Prefecture in 1984 (1) and conducted an experimental work in a wind-wave tank (2). Furthermore, we investigated the characteristics of the internal seiche generated by variable wind stress and its analysis.

RESPONSE SOLUTION OF INTERNAL SEICHE TO WIND

A narrow rectangular closed basin in a two-layered stratified density was chosen as the subject of investigation. We consider the case in which the wind begins to blow with a constant strength in the longitudinal direction over the still water surface. When it finally reaches a steady state after long time, the water surface inclines inversely to interface due to the action of thrusting aside from wind stress. In the upper layer the circulating flow which consists of favorable current near the water surface and adverse current near the interface is formed. The internal seiche exists as the transitional phenomenon in the process shifting to this steady state (2),(4). The oscillation of the interface due to the internal seiche is a standing wave, of which the neutral axis is the final inclined interface and both sides are loop. The wave height of the internal seiche rapidly damps because of the resistance of the interface and only the steady circulating flow appears to remain in the upper layer. If the wind stress on the water surface changes into another strength, the internal seiche occurs again in the process shifting to a steady state for this stress. Therefore, if the wind stress changes successively, then the internal seiche changes the wave height and wave form responding to the wind stress.

The internal seiche is a damping oscillation controlled by the wind stress as the motive force, the inertia force, the restoration force of pressure gradient according to the inclination of, water surface, interface and the friction force on the interface and the bottom. Here, we assume that the internal seiche can be treated the same as the long wave of small amplitude and the phenomenon is linear approximately. Then, we find the impulse response function of the internal seiche to the instantaneous rise in the wind stress, we can obtain the response to the variable wind stress by the principle of superposition. This method was used by Heaps and Ramsbottom (4) to explain the internal seiche observed in a two-layered lake. However, they considered only the resistance of the bottom and disregarded the wind-driven circulating flow in the upper layer and the interfacial resistance which play an important role. Here we derive the response function of internal seiche including the interfacial resistance, based on the theory of Heaps et al.

Interfacial resistance of two-layered flow

The model of flow, the coordinate systems and the used symbols are shown in Fig.1. The wind-driven circulating flow, u_s, of the upper layer in the steady state are typically described in the figure. Wu (19) and Ura (17) made the two-layered flow with salt water and fresh water in a wind-wave tank and measured the circulating flow in the upper layer generated by a constant wind. Ura (17) indicated that the velocity on the interface, u_{si}, is in the direction opposite to the wind and $u_{si}=-1.85u_*$, in which $u_*=\sqrt{\tau_a/\rho_1}$ is the friction velocity on the water surface and ρ_1 is the water density of the upper layer.

The wind-driven flow in a homogeneous lake is a phenomenon provided by the wave velocity $\sqrt{gh}$, but the flow caused by the internal seiche in a two-layered basin is a phenomenon provided by $\sqrt{\varepsilon gh}$, in which g is the gravity acceleration and $\varepsilon=(\rho_2-\rho_1)/\rho_2$. Therefore, it is considered that the wind-driven steady velocity on the interface

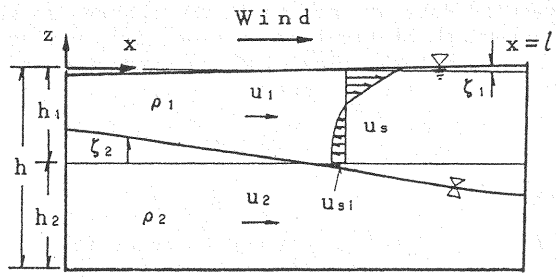

Fig.1 A longitudinal section of the two-layered lake while the water in motion. u_s is the velocity of the steady wind-driven current. u_1, u_2 are the currents caused by the internal seiche.

u_{si} is established before the flow caused by the internal seiche begins to oscillate. Consequently, the relative velocity u_r, which provides the interfacial shear stress T_i of the internal seiche, is given as

$$u_r = u_1+u_{si}-u_2 = (u_1-u_2)-1.85u_* \qquad (1)$$

where u_1 and u_2 are the currents of the upper and lower layers due to the internal seiche, respectively.

Next, in the interfacial resistance expression $T_i/\rho=(f_i/2)|u_r|u_r$, f_i is expressed as a function of Iwasaki's number $\Psi=(h_1u_r/\nu)(u_r^2/\varepsilon gh_1)=u_r^3/\nu\varepsilon g$ shown in Fig.2 in which ν is the kinematic viscosity. Kaneko's expression (9) $f_i=0.2\Psi^{-1/2}$, is shown by the dotted line in the same figure, has often been used for practical use. On the other hand, Ura et al. (18) obtained a semi-theoretical expression, by measuring the flow and turbulence near the interface where the interfacial wave was generated. Their result is shown by the one point chain line in the same figure. In their expression, f_i is rather a curve which is almost proportional to Ψ to the power -1/3 and -1/2 where in $10^2\leqq\Psi\leqq3\times10^4$ and $\Psi\geqq10^5$ respectively. Hino et al. (5) shows f_i, as a ratio of two parameters (u_{si}/u_{s1}), the interfacial velocity u_{si} to the mean velocity u_{s1} of the upper layer flow, and the internal Froude number $F_i=u_{s1}/\sqrt{\varepsilon gh_1}$. At $u_{si}/u_{s1}=0.6$ and $F_i=1.0$, f_i is shown as the two point chain line in the same figure. Nakano et al. (13) proposed a similar expression of Hino et al. (15).

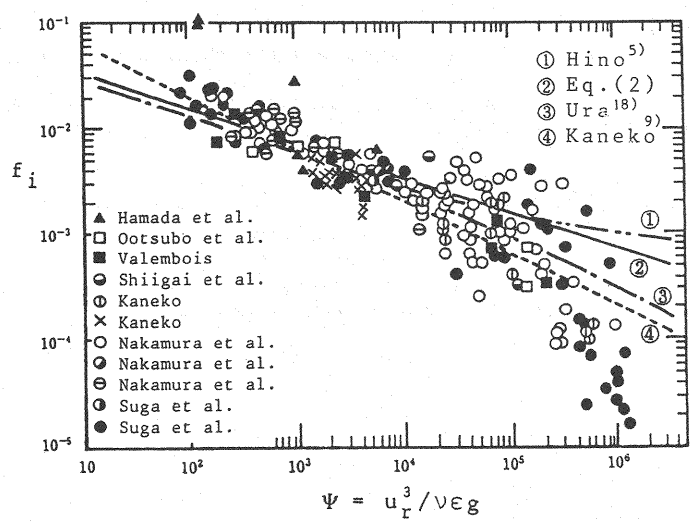

Fig.2 Coefficient of the internal resistance(6)

In Fig.2, the measured data are scattered remarkably, so it is not clear in detail. However, each semi-theoretical expression of f_i varies with gentler slope of Ψ to the power -1/2. Therefore, the following expression of f_i shown by the solid line in the same figure is used here.

$$f_i=0.07\Psi^{-1/3}$$
$$T_i/\rho=0.035(\nu\varepsilon g)^{1/3}u_r \tag{2}$$

Moreover, the bottom friction T_b/ρ_2 is assumed to be as follows:

$$\frac{T_b}{\rho_2} = \frac{n_M^2 g}{h_2^{1/3}}|u_2|u_2 \tag{3}$$

where n_M is the Manning's roughness coefficient.

Response solution of internal seiche

If the internal seiche is regarded as a long wave with small amplitude, the fundamental equations of motion and continuity in the upper and lower layers reduce to:

$$h_1\frac{\partial u_1}{\partial t} = -gh_1\frac{\partial \zeta_1}{\partial x} + \frac{1}{\rho_1}(T_s-T_i) \tag{4}$$

$$h_2\frac{\partial u_2}{\partial t} = -\varepsilon gh_2\frac{\partial \zeta_2}{\partial x} - gh_2\frac{\rho_1}{\rho_2}\frac{\partial \zeta_1}{\partial x} + \frac{1}{\rho_2}(T_i - T_b) \tag{5}$$

$$h_1\frac{\partial u_1}{\partial x} + \frac{\partial \zeta_1}{\partial t} - \frac{\partial \zeta_2}{\partial t} = 0 \tag{6}$$

$$h_2\frac{\partial u_2}{\partial x} + \frac{\partial \zeta_2}{\partial t} = 0 \tag{7}$$

where ζ_1 and ζ_2 are elevations of the water surface and the interface measured from their mean level respectively. T_s, T_i and T_b are the shear stress on the water surface, interface and bottom respectively.

Here, we consider the case in which the wind begins to blow over the water surface at time t=0 and the distribution of wind stress is given as

$$T_s/\rho_1 = H(t)A_n'\sin(n\pi x/l) \tag{8}$$

where H(t) is Heaviside's unit function, n a positive integer and A_n' an amplitude of the wind stress changing in the x direction.

Further, we introduce the following functions as the solutions to the internal seiche satisfying the boundary conditions at both sides, x=0 and x=l.

$$\zeta_1 = Z_1(t)\cos(n\pi x/l)$$
$$\zeta_2 = Z_2(t)\cos(n\pi x/l)$$
$$u_1 = U_1(t)\sin(n\pi x/l) \tag{9}$$
$$u_2 = U_2(t)\sin(n\pi x/l)$$
$$u_* = U_{*n}\sin(n\pi x/l)$$

where Z_1, Z_2, U_1, U_2 and U_{*n} are the amplitudes of ζ_1, ζ_2, u_1, u_2 and u_* changing in the x-direction, respectively. Using Eqs.1 to 3, and $\rho_m=(\rho_1+\rho_2)/2$ the shear stress on the interface and the bottom can be obtained as

$$T_i/\rho_m = 2f(u_1-u_2-1.85u_*) \tag{10}$$

$$T_b/\rho_2 = 2ku_2 \tag{11}$$

where

$$2f = 0.035\,(\nu\varepsilon g)^{1/5}$$
$$2k = n_M^2 g h_2^{-1/3}|u_2| \tag{12}$$

It will be shown later that the influence of the coefficient 2k of the bottom resistance is negligible compared with that of the coefficient 2f of the interface resistance. Here we treated 2k as a constant in the following way.

First, we introduce the non-dimensional quantities as follows:

$$\begin{aligned} x/l &= \xi\,, & t/(l/\sqrt{gh}) &= \tau \\ gZ_1/u_*^2 &= \eta_1\,, & gZ_2/u_*^2 &= \eta_2 \\ U_1/u_* &= \upsilon_1\,, & U_2/u_* &= \upsilon_2 \\ f/u_* &= \tilde{f}\,, & k/u_* &= \tilde{k} \\ A_n'/u_*^2 &= A_n\,, & B_n'/u_*^2 &= B_n \end{aligned} \tag{13}$$

where $B_n'=2f\times 1.85U_{*n}$. Substituting Eqs.8 to 13 into Eqs.4 to 7, then taking the Laplace transforms

$$\bar{\eta} = \int_0^\infty e^{-s\tau}\eta(\tau)d\tau$$

where the transformed quantities denoted by the overbar, we have

$$\begin{aligned} &\frac{\sqrt{gh}}{u_*}\frac{h_1}{l}s\bar{\upsilon}_1 = \frac{n\pi h_1}{l}\bar{\eta}_1 + (A_n+B_n)\frac{1}{s} - \frac{\rho_m}{\rho_1}2\tilde{f}(\bar{\upsilon}_1-\bar{\upsilon}_2) \\ &\frac{\sqrt{gh}}{u_*}\frac{h_2}{l}s\bar{\upsilon}_2 = \frac{n\pi h_2}{l}\left(\frac{\rho_1}{\rho_2}\bar{\eta}_1 + \varepsilon\bar{\eta}_2\right) - 2\tilde{k}\bar{\upsilon}_2 + \frac{\rho_m}{\rho_2}2\tilde{f}(\bar{\upsilon}_1-\bar{\upsilon}_2) - B_n\frac{1}{s} \\ &\frac{\sqrt{gh}}{u_*}n\pi\frac{h_2}{h}\bar{\upsilon}_1 + s\bar{\eta}_1 - s\bar{\eta}_2 = 0 \\ &\frac{\sqrt{gh}}{u_*}n\pi\frac{h_2}{h}\bar{\upsilon}_2 + s\bar{\eta}_2 = 0 \end{aligned} \tag{14}$$

These simultaneous linear equations for $\bar{\upsilon}_1$, $\bar{\upsilon}_2$, $\bar{\eta}_1$ and $\bar{\eta}_2$ can be solved easily, but the obtained solutions are so complex that we can not directly take their inverse Laplace transformation. However, an approximation of $\rho_1/\rho_2=\rho_m/\rho_1=\rho_m/\rho_2=1$ and omitting the former term of the factor $(\tilde{k}+\tilde{f}(h/h_1)^2)$ included in the equations of $\bar{\eta}_1$ and $\bar{\eta}_2$ (the values of $\tilde{k}$ and $\tilde{f}$ will be shown later), we can obtain the functional forms in order to find the inverse Laplace transformation. After the cumbersome calculations, the elevations η_1 and η_2 are given as

$$\begin{aligned} \eta_1 = &-\frac{1}{n\pi h_1}\Big[(A_n+B_n) - A_n\frac{h_1}{h}\Big\{\cos(n\pi\sigma_{1n}\tau) + \frac{3\alpha_1}{n\pi\sigma_{1n}}\sin(n\pi\sigma_{1n}\tau)\Big\}e^{-\alpha_1\tau} \\ &- A_n\frac{h_2}{h}\Big\{\cos(n\pi\sigma_{2n}\tau) + \Big(\tilde{f}\frac{h^2}{h_1^2} - \tilde{k}\Big)\frac{1}{n\pi\sigma_{2n}}\frac{h_1}{h_2}\frac{u_*}{\sqrt{gh}}\frac{1}{h}\sin(n\pi\sigma_{2n}\tau)\Big\}e^{-\alpha_2\tau} \\ &- B_n\Big\{\cos(n\pi\sigma_{2n}\tau) + \frac{\alpha_2}{n\pi\sigma_{2n}}\sin(n\pi\sigma_{2n}\tau)\Big\}e^{-\alpha_2\tau}\Big] \end{aligned} \tag{15}$$

$$\eta_2 = \frac{1}{n\pi h_1}\frac{1}{\varepsilon}(A_n + \frac{h}{h_2}B_n)\left[\ 1 - \left\{ \cos(n\pi\sigma_{2n}\tau) + \frac{\alpha_2}{n\pi\sigma_{2n}}\sin(n\pi\sigma_{2n}\tau)\right\} e^{-\alpha_2\tau}\right]$$

where (16)

$$\begin{aligned}
\alpha_1 &= \tilde{k}\frac{u_*}{\sqrt{gh}}\frac{1}{h} \\
\sigma_{1n}^2 &= 1 - (\alpha_1/n\pi)^2 \\
\alpha_2 &= (\tilde{f}\frac{h^2}{h_1^2} + \tilde{k})\frac{u_*}{\sqrt{gh}}\frac{h_1}{h_2}\frac{1}{h} \\
\sigma_{2n}^2 &= \varepsilon h_1 h_2/h^2 - (\alpha_2/n\pi)^2
\end{aligned} \qquad (17)$$

Eqs.15 and 16 are solutions to the case of σ_{1n}^2 , $\sigma_{2n}^2 > 0$. If the resistance of the interface and bottom are large and σ_{1n}^2, $\sigma_{2n}^2 < 0$, the trigonometric functions in the equations become the hyperbolic functions, with no oscillations the flow asymptotically shifts to the steady state having the slope of the water surface and interface in accordance with the wind stress. However, in the actual water area, Eq.17 which represents σ_{1n}^2 and σ_{2n}^2, each 2nd term is very small in comparison with the 1st term.

The currents υ_2 and υ_1 generated by the internal seiche are obtained easily from the equations of continuity, Eqs.7 and 6, as follows:

$$\begin{aligned}
\upsilon_2 &= -\frac{1}{n\pi}\frac{u_*}{\sqrt{gh}}\frac{h}{h_2}\frac{d\eta_2}{d\tau} \\
&= -\frac{1}{\varepsilon}(A_n + \frac{h}{h_2}B_n)\frac{u_*}{\sqrt{gh}}\frac{h^2}{h_1 h_2}\frac{1}{h}\frac{\sigma_{2n}}{n\pi}\left\{1 + (\frac{\alpha_2}{n\pi\sigma_{2n}})^2\right\}\sin(n\pi\sigma_{2n}\tau)e^{-\alpha_2\tau}
\end{aligned} \qquad (18)$$

$$\upsilon_1 = \frac{1}{n\pi}\frac{u_*}{\sqrt{gh}}\frac{h}{h_1}(-\frac{d\eta_1}{d\tau} + \frac{d\eta_2}{d\tau}) = -\frac{1}{n\pi}\frac{u_*}{\sqrt{gh}}\frac{h}{h_1}\frac{d\eta_1}{d\tau} - \frac{h_2}{h_1}\upsilon_2 \doteqdot -\frac{h_2}{h_1}\upsilon_2 \qquad (19)$$

Eqs.15 to 19 give the response solutions in the motion of the lake generated by the wind stress in Eq.8.

Here, consideration of the more general case in which the wind stress over the water surface is arbitrarily distributed in the x-direction is taken as

$$T_S/\rho_1 = H(t)A'(x) \qquad (20)$$

where A'(x) is any distributed function of x ($0<x<1$) which may be represented as a Fourier series:

$$\begin{aligned}
A'(x) &= \sum_{n=1}^{\infty} A'_n \sin(n\pi x/l) \\
(A'_n &= \frac{2}{l}\int_0^l A'(x)\sin(n\pi x/l)dx)
\end{aligned} \qquad (21)$$

The flow system is regarded linear and so the response to this wind can be obtained by the sum of the responses of each component of the wind (each term of Fourier series). If we rewrite $Z_1(t)$ and $U_1(t)$ etc. of Eq.9 in terms of $Z_1(n,t)$ and $U_1(n,t)$ etc. in order to represent the response function of each component, the responses to wind in Eqs.20 and 21 are obtained by the following.

$$\begin{aligned}
\zeta_1 &= \sum_{n=1}^{\infty} Z_1(n,t)\cos(n\pi x/l) \\
\zeta_2 &= \sum_{n=1}^{\infty} Z_2(n,t)\cos(n\pi x/l) \\
u_1 &= \sum_{n=1}^{\infty} U_1(n,t)\sin(n\pi x/l) \\
u_2 &= \sum_{n=1}^{\infty} U_2(n,t)\sin(n\pi x/l)
\end{aligned} \qquad (22)$$

These expressions give the elevations(ζ_1,ζ_2) of the water surface and interface as well as the currents(u_1,u_2) of the upper and lower layers generated by the steady wind stress. On the basis of these solutions, we consider the response of the lake of the general case in which the strength of the wind stress varies with time. We assumed that the profile of the wind stress distribution above the water surface does not change and its strength varies with time only, and the wind stress represented as

$$T_s/\rho_1 = \vartheta(t)A'(x) \qquad (t>0) \tag{23}$$

We consider the response of water surface elevation $d\zeta_1$ at time t to the rectangular pulse wind stress shadowed in Fig.3. The rectangular pulse can be regarded as the condition that the wind stress rises stepwise with the strength ϑ at time t' and with the strength $(-\vartheta)$ at time t'+dt'. If ζ_1' denotes the response to unit wind stress stepwise, we have

$$d\zeta_1 = \vartheta(t')\zeta_1'(t-t') - \vartheta(t')\zeta_1'(t-(t'+dt'))$$

If we regard the wind stress to vary with time as shown in Fig.3 as a series of steps:

$$\begin{aligned} \vartheta(t') &= \vartheta_1 && (\ 0 \leqq t' < t'_1\ ) \\ &= \vartheta_2 && (\ t'_1 \leqq t' < t'_2\ ) \\ &= \vartheta_3 && (\ t'_2 \leqq t' < t'_3\ ) \\ &\ \ \vdots \end{aligned}$$

the response at time t is given by the total sum of the responses to each pulse from time t'=0 to time t'=t as

$$\begin{aligned} \zeta_1 = {} & \vartheta_1\zeta_1'(t) + (\vartheta_2-\vartheta_1)\zeta_1'(t-t') \\ & + (\vartheta_3-\vartheta_2)\zeta_1'(t-t'_2) + \cdots + (\vartheta_{i+1}-\vartheta_i)\zeta_1'(t-t'_i) \end{aligned} \tag{24}$$

Substituting ζ_2', u_1', u_2' instead of ζ_1' in Eq.24, we can obtain the other response ζ_2, u_1, u_2 to the successive variable wind.

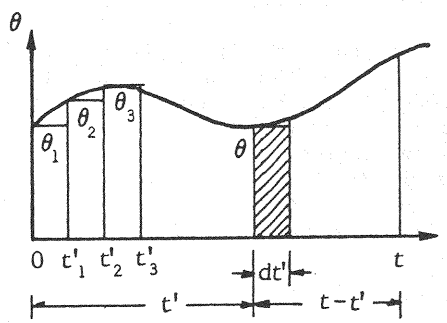

Fig.3 Variable wind stress with the passage of time

EXPERIMENT OF INTERNAL SEICHE BY THE WIND-WAVE TANK

The experiment and its apparatus

The experiments were performed in a wind-wave tank, as shown in Fig.4, 6.00m in

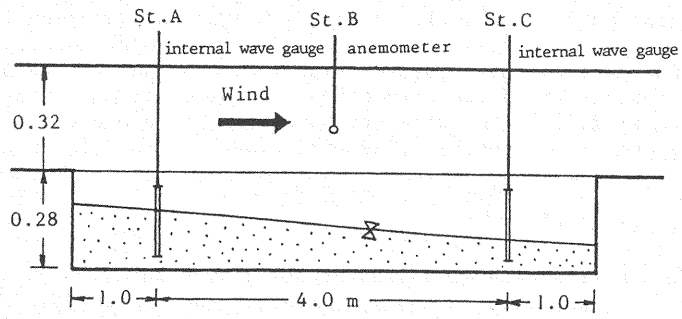

Fig.4 Experimental flume with wind tunnel

length, 0.28m in depth and 0.30m in width, the upper part of which was the wind channel of the same width and 0.32m in height. In the blower side it was provided with the rectifying wind channel 4m in length, which had the same section as the wind channel above the water tank. After making two-layered stratifications by floating tap water carefully above the salt water of a uniform density (in the experiments, ρ_2=1.008~1.025g/cm^3), the wind was fanned by the blower and the variation of interfacial level was measured. Moreover, in order to obtain the conditions of the density stratification, the density distribution was measured by salinometer, at one section in the water tank before the start and after the ending of the experiment, when the water in the tank was quieting down. Measurement at the three sections A, B and C as shown in Fig.4 were done during the experiment of ventilation.

The interfacial displacement was measured by the internal wave gauge with resistant wire set up at the two stations of A and C 1m away from both sides of the water tank. Because the rotation of blower was not variable, the wind velocity was varied by changing the opening of the blower valve in steps and was measured by the anemometer provided at a height of 10cm above the water surface in the center (St.B) of the water tank. Wind stress T_a on the water surface was evaluated by measuring the wind velocity distribution near the water surface in detail before the variation of the winds opening of the blower valve to obtain the relation between the wind stress T_a and the representative wind velocity U_{ma}. These measurements was done at a height 10cm above the water surface. Further, the wind stress in regular experiment of the variable wind was obtained from measured U_{ma} and the relation between T_a and U_{ma}.

The experimental results and its considerations

a)The wind stress on the water surface and the flow conditions

To evaluate the wind stress on the water surface, the ordinary method was used in experiment, which is to apply the measured wind distribution near the water surface to the logarithmic rule and then calculated backwards. The wind distributions for various openings of the blower valve are plotted on semi-logarithmic paper as shown in Fig.5. The wind velocity in a height more than 10cm is almost uniform, but the plots of the wind velocity near the water surface are approximately a straight lines in semi-logarithmic paper and conform to the logarithmic rule which is:

$$\frac{u_a}{u_{*a}} = \frac{2.30}{\varkappa} \log(z/z_0) \qquad (25)$$

where u_a is the wind velocity at a height z above the water surface, u_{*a} the friction velocity of the wind, $\varkappa$ the von Kármán's constant(=0.4) and z_0 the roughness length. u_{*a} is calculated backwards for the straight lines in Fig.5 by

using Eq.25. These values are plotted to the representative wind velocity U_{ma} in Fig.6. The wind stress on the water surface is given as

$$T_a = \rho_a u_{*a}^2 \qquad (26)$$

where ρ_a is the air density.

Further, the wind distributions were measured at stations A, B and C as shown in Fig.4 and then we obtained u_{*a} at each station. However, a significant difference at each station was not recognized. Thus, the uniform wind stress acting on the water surface in the water tank was regarded.

If the wind blows with a constant strength continuously, the interface rises on the windward side and falls on the lee side, and inclines with the slope according to the wind stress, and the steady circulating flow is formed in the upper layer as shown in Fig.1 typically. In the process of shifting to a steady state, the internal seiche generated in the water tank is one node standing wave to be loop at both sides and node at the center, which oscillates about a steady interface position. Therefore, the flow of internal seiche is considered to be composed of the uniform reciprocating flows in the upper and lower layers, which are mutually in the opposite direction, and a steady circulating flow. These flow conditions are included in the expressions of the interfacial resistance and the bottom resistance given in Eqs.10 and 11.

The steady circulating flow of the upper layer near the interface is in the opposite direction to the wind and carries the interfacial mixing water to the windward. Thus, with the passage of time the thickness of layer of discontinuity becomes thick at the windward side but thin at the lee side.

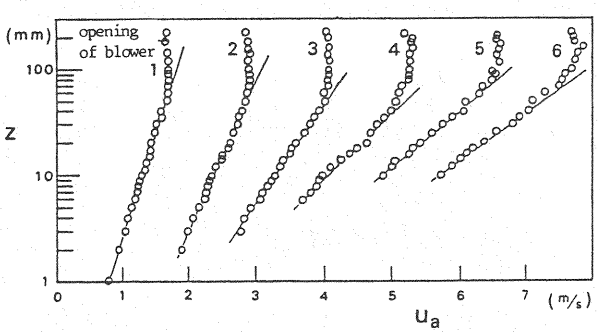

Fig.5 Velocity distribution of the wind above the water surface at St.B of the wind tunnel flume.

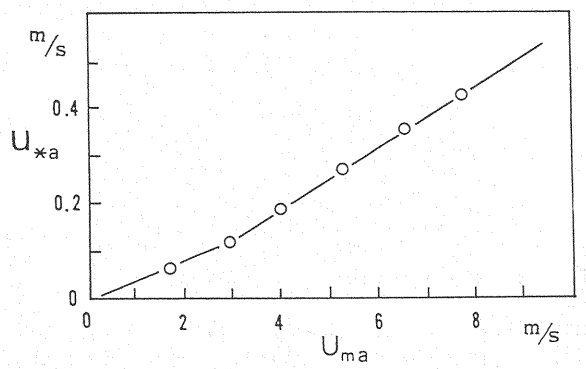

Fig.6 Relation between representative wind velocity and wind friction velocity.

b)The interfacial oscillation and its simulation

The interfacial displacement was measured by the internal wave gauge at St. A and C shown in Fig.4. One example of the experimental results is shown in Fig.7. The wind speed in experiment was changed in steps at 8 ~ 9 minutes intervals. Fig.7 shows clearly the behavior of generation and damping of the internal seiche and the variation of the wave height accompanied with the changing in the wind speed. Moreover, we can find that the inclination of the mean interface, which is a center position of the oscillation, is completed rapidly after the changing in the wind speed.

The changing in the interfacial displacement is simulated by using the response solutions and the method of superposition. First, we obtain the wind stress on the water surface from the measured wind speed U_{ma}, Fig.6 and Eq.26. The water surface stress T_s is almost equal to the wind stress T_a on the water surface, so that

$$T_a = T_s = \rho_1 u_*^2 \tag{27}$$

Furthermore, T_s can be regarded as a uniformly distributed throughout the water surface so that the Fourier series expression on T_s is given as

$$T_s/\rho_1 = H(t) \sum_{n=1}^{\infty} \frac{4}{n\pi} u_*^2 \sin(n\pi x/l) \tag{28}$$

(where, $n=1,3,5,\cdots$)

Therefore, in this case A_n and B_n are treated as

$$A_n = (4/n\pi) \quad , \qquad B_n = (2\tilde{f}\times 1.85)(4/n\pi)$$

In this case, we can rewrite Eq.22 of ζ_2. Omitting the sin term in Eq.16 because the coefficient multiplied by the sin is very small compared to unity and neglecting the second term in σ_{2n}^2 of Eq.17, we obtain from Eq.16, 17 and 22 the following:

$$\frac{g\zeta_2}{u_*} = \eta_{2a} \sum_{n=1}^{\infty} \frac{4}{n^2\pi^2} \cos(n\pi\xi)\{1-\cos(n\pi\sigma_2\tau)e^{-\alpha_2\tau}\}$$

$$= \eta_{2a}\{(\frac{1}{2}-\xi) - \frac{\pi\pm\Theta\pm\Theta'}{2\pi} e^{-\alpha_2\tau}\} \tag{29}$$

$(n=1,3,5\cdots)$

wherein,

$$\sigma_2 = \varepsilon h_1 h_2/h^2$$

$$\eta_{2a} = \frac{1}{\varepsilon h_1}\{1+(2\tilde{f}\times 1.85)\frac{h}{h_2}\}$$

$$\Theta = \pi(\xi+\sigma_2\tau)$$

$$\Theta' = \pi(\xi-\sigma_2\tau)$$

In Eq.29, the positive sign of Θ and Θ' is taken as $-\pi \leqq \Theta$ (or Θ') $\leqq 0$ and negative sign for $0 \leqq \Theta$ (or Θ') $\leqq \pi$.

The oscillating shape of the interfacial displacement given by Eq.29 is shown in Fig.8. But, the wave shown in this figure is a fundamental wave that is accompanied with no damping($\alpha_2=0$) at station $\xi(=0.7)$. The actual wave shows a damping oscillation of which the neutral position is located at the dotted line of this figure and the amplitude damps exponentially with time.

It is found from Fig.8 that the internal seiche oscillates has a period of about $\pi\sigma_2\tau=2\pi$. Therefore, the oscillating period T is given by

$$T = 2l/\sqrt{\varepsilon g h(h_1 h_2/h^2)} \tag{30}$$

When $\tau=\infty$ in Eq.29, the final form of the interface is obtained as a straight line to ξ. The gradient of interface is given by

$$\frac{d\zeta_2}{dx} = -\left\{1+(2\tilde{f}\times 1.85)\frac{h}{h_2}\right\}\frac{u_*^2}{\varepsilon g h_1} \tag{31}$$

This equation agrees with the equation of interfacial gradient which is derived from the balance of the forces composed of wind stress on the water surface $T_s/\rho_1=u_*^2$ and interfacial friction $T_i/\rho_m=-2f\times 1.85u_*^2$.

The result of the calculated simulation of the experiment is shown in Fig.7. According to this figure the calculated wave heights are a little larger than measured, but the variation of wave heights accompanied with the changing in wind velocity and the damping of wave heights are expressed almost correctly. Therefore the validity of the theoretical solutions and the technique of calculation can be admitted. In this experiment, the value of f given by Eq.12 becomes $f=1.0\times10^{-4}$ m/s, and if Manning's roughness coefficient is assumed to be $n_M=0.01$ and $u_2=0.01$m/s, then the value of k becomes $k=0.009\times10^{-4}$m/s. Thus, the bottom resistance can be disregarded compared with the interfacial resistance.

Moreover, each second term of σ_{1n}^2 and σ_{2n}^2 in Eq.17 is minute compared with each of the first terms, so both terms can be disregarded.

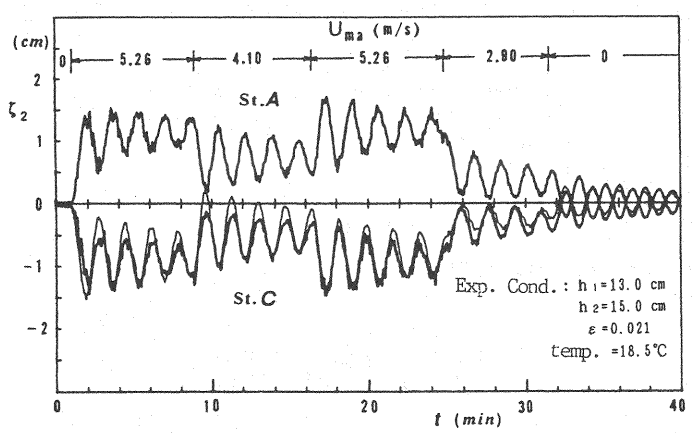

Fig.7 Interfacial elevations ζ_2 at St.A and C corresponding to wind velocity U_{ma} (the thick line shows the experimental results and fine line by simulation).

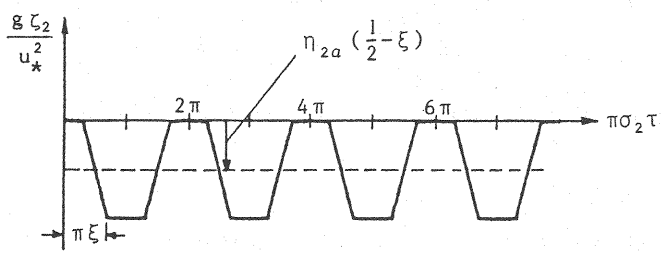

Fig.8 Oscillation of ζ_2 given by Eq.29 ($\alpha_2=0$)

THE INTERNAL SEICHE IN OHNO RESERVOIR BY THERMAL STRATIFICATION

Ohno Reservoir and the field observation

Ohno Reservoir, is located at the north slope of Mt. Daisen, 480m above sea level, in Tottori Prefecture. It is used mainly for irrigation purposes and small in size as shown in Fig.9. It is 1.1km in circumference, with a total storage capacity of $1.19\times10^5m^3$. The water surface area of the reservoir is $5.3\times10^4m^2$ with a mean depth of 2.26m. A very little water flows into the reservoir from the ground surface, and this reservoir is filled with relatively cold water springing from the bottom (the water temperature is 14 °C and the spring rate is $0.08m^3/s$). Consequently, for this reservoir size the stratification of the water temperature appears remarkably in summer season, due to stabilization of the atmospheric pressure pattern during this time of the year. The wind direction is so separated that the valley wind blows from the north in daytime while a mountain wind from the south in nighttime. As the prominent direction of wind agrees with the longitudinal axis of this reservoir, the internal seiche can be observed frequently in summer season.

To observe the internal seiche responding to the wind, we conducted the field observation of the water temperature, the wind direction, the wind velocity, etc. continuously from the 3rd to the 6th of August 1984. We measured the water temperature for 12 fixed depths at each station A, B and C shown in Fig.9. In each station, the thermocouples were suspended from a fixed buoy to 2.4m in depth with a space of 20cm vertically. The water temperature for a total of 36 points were recorded almost simultaneously at 1 minute interval (the switching time between sensors was 0.1 second).

Wind direction and wind velocity were measured by propeller anemometer provided at a height of 1.64m above the water surface at station B, wherein the wind direction and the velocity averaged for one minute were recorded, too. Moreover, the atmospheric temperature was measured at a height of 20cm above the water surface in station B simultaneously. All measured items were recorded on a digital tape recorder at one minute interval.

For observation period, the weather was almost fine, but there was a light rain from 12 to 14 o'clock on the 5th of August. The discharge corresponding to the spring water was always overflowing through the spillway weir in the northern end of the reservoir.

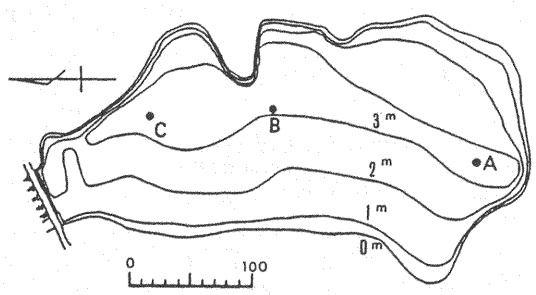

Fig.9 Ohno Reservoir showing the depth contours and the observation stations

The observed results and its considerations

(a)The wind stress and the changing in the water temperature

The conditions of stratification is shown in Fig.10. This is the vertical distribution of the water temperature at the three stations A, B and C at 0:00 on the 5th of August when the reservoir was calm. There is isothermal surface layer which is from the water surface to a depth of 0.8m, followed by a thermocline

layer to the bottom where the water temperature falls almost linearly. There is no hypolimnion layer because this reservoir is shallow.

The time series of the wind velocity andthe wind direction for two days of the observation and the calculated wind stress on the water surface (component in the south direction) are shown in Fig.11. It was a weak wind comparatively and the wind velocity was less than 4m/s. There were two patterns of the wind direction, it blew from the north in the daytime and from the south in the nighttime. It seemed that a disturbance in the atmospheric pressure passed from 15 to 16 o'clock on the 5th, so that the wind velocity became strong lightly with simultaneous changes in the wind direction from the north to the south and there was a light rain.

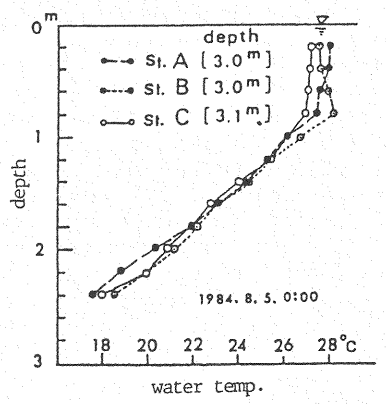

Fig.10 Vertical distributions of the temperature at St.A, B and C of Ohno reservoir : 0:00 5th August 1984.

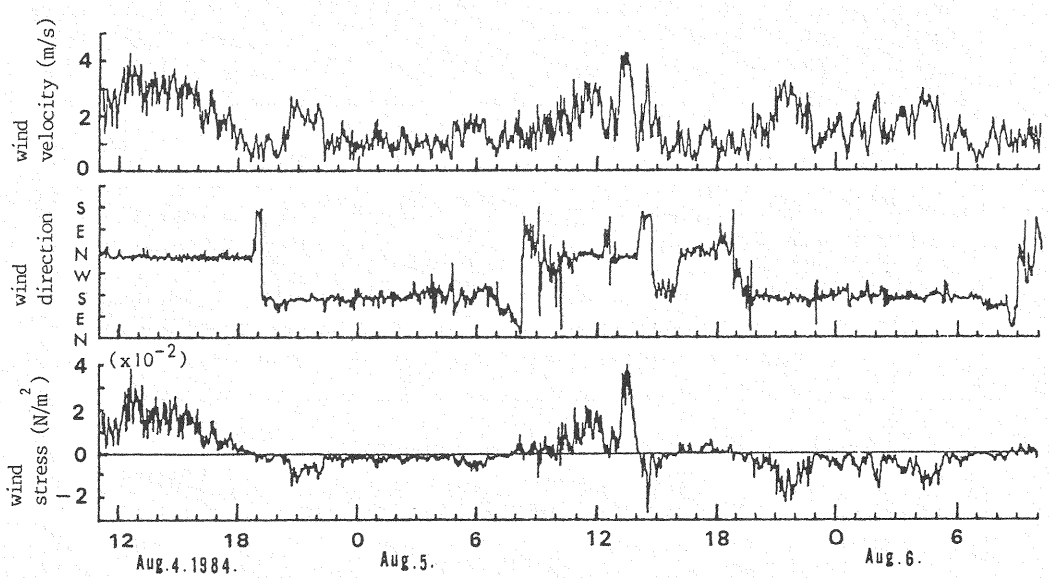

Fig.11 Time series of wind velocity, the wind direction observed at St.B, and the wind stress (southern direction component) calculated using Eq.32.

Wind stress on the water surface was obtained by the following calculation. The relation between the coefficient of resistance C_D on the water surface and the wind velocity U_{10}(wind velocity at 10m in height above the water surface) is summarized by Phillips (14). C_D is a constant value of about 0.9×10^{-3} for a weak wind less than 5m/s according to him. Therefore, T_a was calculated using the expression:

$$T_a = \rho_a C_D U_{10}^2 \ ; \quad C_D = 0.9\times10^{-3} \qquad (32)$$

The wind velocity U_{10} was converted from the wind velocity measured at 1.64m in height using Eq.32 and the logarithmic rule of wind velocity. The wind stresses shown in Fig.11 are the components in the south direction which are the products of T_a and the cosine of the azimuch of the wind direction.

Time series of the water temperature measured for each depth at the three stations A, B and C are shown in Fig.12. The water temperature of the surface layer, from the water surface to a depth of 0.8m changes at a range of about 2°C in the diurnal period and so it appears to be caused by the heat transfer from the water surface by sunlight. The water temperature in a layer below 1.4m in depth changes in a much shorter period than diurnal period. This consideration is that the layer below 1.4m is almost independent of the water temperature from the surface layer and the change in the water temperature has been caused by the current due to wind such as the internal seiche. Especially, after the blowing of the wind on the 5th of August at 13:00, the water temperature oscillates at large amplitude with a period of above 2 hours. In addition, the amplitudes of oscillation at stations A and C are large considerably compared with that at station B.

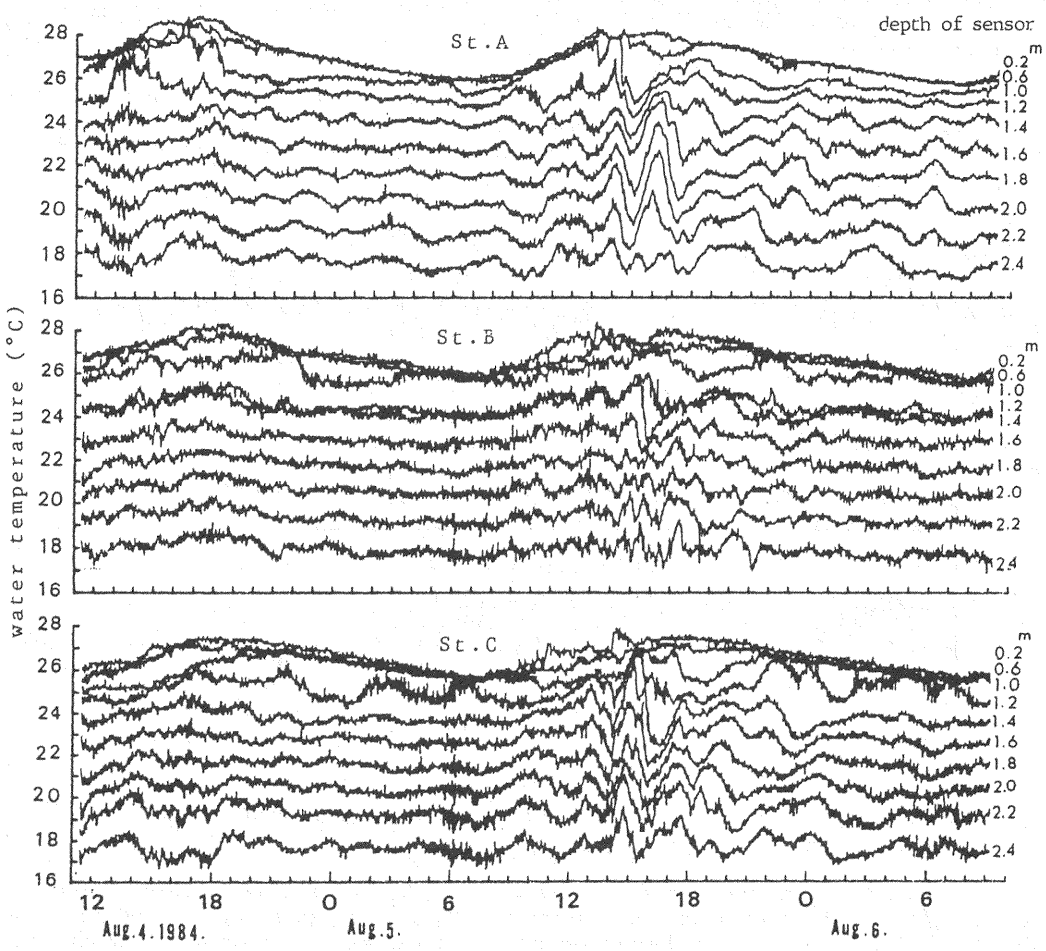

Fig.12 Time series of the water temperature observed for each depth at St.A, B and C.

Next, we transform the wave of the water temperature to the vertical displacement of water particle. As the vertical distribution of water temperature is almost linear below the surface layer, the water temperature is assumed to be changing lineary between two thermo-sensors which are provided at 20cm intervals, and then the depth of the desired temperature is calculated by interpolation. The changing in depth of this isothermal layer (vertical displacement of isothermal layer) is almost a reverse shape of the shape of the vertical temperature wave in

Fig.12. The changing in the depth of isothermal layer, in which the water temperature is 22°C at stations A, B and C from 7:00 on the 5th to 3:00 on the 6th of August, is shown in Fig.13. To avoid the overlapping of lines, the lateral axis of time is common, but the vertical axes are drawn to be a little shifted mutually. In this figure, if we compare station A with C, the phases of waves are perfectly reversed mutually, and therefore when the displacement of one side is positive, the another side is negative. Moreover, the amplitude of displacement at station B is considerably small compared with that at stations A and C. According to the fact as mentioned above, it is understood that the oscillation of isothermal layer shows the internal seiche in which the center of reservoir is a node and both sides are loop in longitudinal axis direction.

(b)Auto-correlation function, spectrum of the vertical displacements of the isothermal layer and the predominant period of the internal seiche

To examine the relation between the period and the magnitude of amplitude of the internal seiche, the auto-correlation function R_j of the time series of the displacement from the mean depth of each isothermal layer was calculated. For the calculations, we used the data of 1024 minutes starting from 7:00 o'clock on the 5th. R_j at stations A and B is shown in Fig.14 and R_j at station C is omitted, because it is almost the same as at station A. According to this figure, R_j at station A is clearly admitted to be periodical but R_j at station B is not. For R_j at station A, except R_j of 18°C and 19°C in the bottom water layer, the lag times of the positive peak correlation appear on the points to be integer multiple of about 2.3 hours, and so it is considered that the predominant period T of internal seiche is about 2.3 hours. Moreover, as far as the value of correlation in lag time of 2.3 hours at station A is concerned, R_j of 21°C and 22°C isothermal layers are the largest. This is considered that in this internal seiche the isothermal layer of 21 or 22°C corresponds to the interface in a two-layerd stratification.

The power spectrum of the time series of the vertical displacement at 22°C isothermal layer at stations A and B is shown in Fig.15. It was calculated by FFT method and used the data of 2048 minutes starting from 18:00 on the 4th. There is a high peak in frequency which is equivalent to period of 2.3 hours at station A and so it is evident that the wave motion due to the internal seiche is prominent. Simultaneously, it is shown that there are peaks to be equivalent to the periods of 1.14, 0.75 and 0.53 hours and the high frequency waves, which have 3 times frequency of the internal seiche predicted theoretically besides 2 or 4 times frequency, are contained.

As mentioned above, it is clear that the internal seiche having a period of 2.3 hours is prominent. This value of the period agrees almost with the theoretical solution of the fundamental period obtained generally for various stratification.

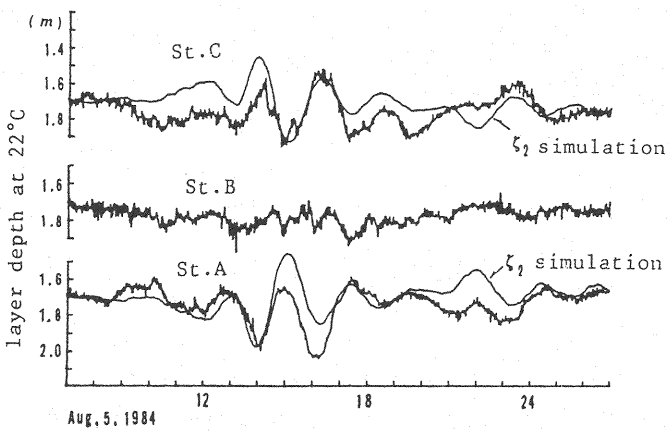

Fig.13 Time variations of the layer depth with temperature 22°C and simulated results at st.A, B and C.

For instance(15), if the Brunt-Väisälä frequency $N=\left[-(g/\rho)(d\rho/dz)\right]^{1/2}$ is taken as a constant in the whole depth and the water density is given by

$$\rho = \rho_0 \exp(-N^2 z/g) \tag{33}$$

then, the fundamental period of the internal seiche in a rectangular lake of a depth h and length l is given by

$$T = 2(l/N)\sqrt{(\pi/l)^2 + (\pi/h)^2} \tag{34}$$

We apply this expression to Ohno reservoir. By assuming ρ_0 to be the water density of a temperature 29°C and $N=0.10s^{-1}$, the distribution of the density corresponding to water temperature shown in Fig.10 can be approximated by Eq.33 without the surface layer. And if l=350m and h=2.8m are assumed, T becomes 2.18 hours.

Moreover, regarding the layer of water temperature at 22°C as the interface and using the values shown in Table 1 and Eq.30 we obtain the fundamental period to be T=2.19 hours. Each theoretical value of fundamental period almost agrees with observed value.

Finally, we calculate the displacement ζ_2 of the interface at stations A and C by the previous mentioned calculation technique under the conditions shown in Table 1. It is assumed that ρ_1 and ρ_2 are water densities equivalent to the temperature 25 and 19°C respectively and the interface is at a depth of 22°C in temperature. The values used for simulation is after 7:00 on the 5th of August and it is assumed that before that time there is no wind and after that time the wind stress shown in Fig.11 acts uniformly on the whole water surface. The simulated results are shown in Fig.13 together with the observed depth at a temperature of 22°C. The observed and the simulated waves are considerably similar, though there are a few difference in the mean levels of the waves, and so this simulating method is admitted to be valid to calculate the response of the internal seiche to the wind. However, the two-layered flow theory is applied to Ohno Reservoir which is stratified continuously and so the range of the replacement of a continuous stratification flow to a two-layered flow must be examined in the future.

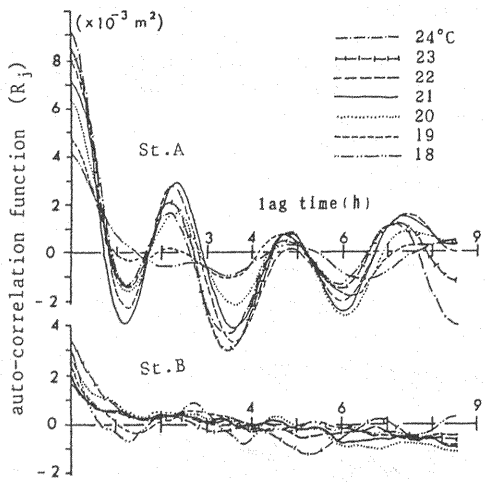

Fig.14 Auto-correlation functions of the time series of the vertical displacement in iso-thermal layer at St.A and B.

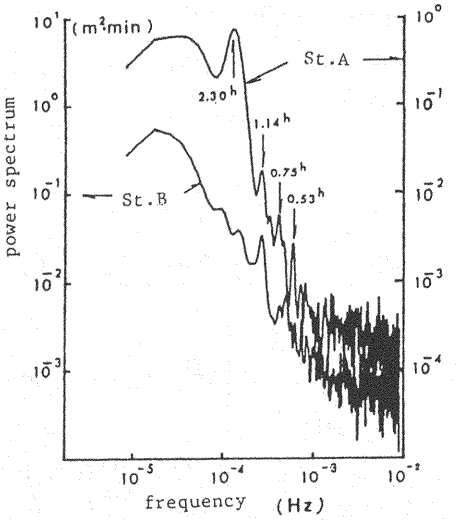

Fig.15 Spectrum of the time series of the vertical displacement in iso-thermal layer with a temperature of 22°C at St.A and B.

Table 1 Values used in the simulation.

l	350 m
h_1	1.7 m
h_2	1.1 m
ρ_1	997.1 Ns^2/m^4
ρ_2	998.3 Ns^2/m^4

CONCLUSION

The behavior of the internal seiche generated by the wind in a closed basin is investigated. The theory is constructed on a basis of a small-amplitude wave theory for two-layered flow in consideration to the interfacial resistance. The theory is applied to simulate the results of a wind-wave tank experiment and a field observation in Ohno Reservoir, and then its validity is made clear. The obtained main conclusions are as follows:

(1)Internal seiche is generated in the process of shifting to a steady state according to the change in wind stress.

(2)Internal seiche oscillates vertically on the inclined interface according to the wind stress and its amplitude decreases rapidly.

(3)The theory of the internal seiche introduced the interface resistance and the bottom resistance is obtained analytically to improve Heaps et al. methods. Also, rapid damping of the internal seiche is caused by the interfacial resistance, and the bottom resistance can be disregarded.

(4)Interfacial oscillation obtained from the field observation shows the complex wave form including the internal seiche and is small-scaled interfacial wave, but the prominent period can be obtained by auto-correlation function and spectrum analysis. Moreover, the interfacial displacement of the internal seiche in the field observation can be explained by numerical simulation calculated using the response functions to the wind with a constant strength.

ACKNOWLEDGMENTS

The authors wish to thanks Professor T. Tsubaki of Kyushu Institute Univ. and Professor Y. Awaya of Kyushu Kyoritsu Univ. for their valuable comments on this study. The authors are also grateful to Mr. K. Ichinose and Mr. Y. Fujikawa of Yachiyo Engineering Ltd. (formerly post-graduate students of Nagasaki Univ.), for their ardent cooperation in the experiment and the field observation.

REFERENCES

1. Furumoto, K., T. Takemasa, K. Ichinose and Y. Fujikawa : Internal seiche in density stratified lake, Proc. 29th Japanese Conf. on Hydraulics, JSCE, pp.389-394, 1985.(in Japanese)
2. Furumoto, K., T. Takemasa, H. Komoda and K. Ichinose : Response of internal seiche to wind in a stratified basin, Proc. 32nd Japanese Conf. on Coastal Engineering, JSCE, pp.722-726, 1985.(in Japanese)
3. Haurwitz, B., H. Stommel and W.H. Munk : On thermal unrest in the ocean, Rossby Memorial Volume, Rockefeller Inst. Press, pp.79-74, 1959.
4. Heaps, N.S. and A.E. Ramsbottom : Wind effects on the water in a narrow two-layered lake, Phil. Trans. Roy. Soc. London, Ser. A, 259 (1102), pp.391-430, 1966.
5. Hino, M. and Nguen son Hung : Velocity distribution interfacial friction and entrainment in two-layered stratified flows, J. Hydrosci. and Hydraul. Eng., JSCE, Vol. 1, No.1, pp.9-36, 1983.
6. JSCE ed. : Formulae in Hydraulics, pp.61.(in Japanese).
7. Kanari, S. : On the studies of internal waves in Lake Biwa(I), Disaster

Prevention Res. Inst. Annuals, No.11, B, pp.179-189, 1968.(in Japanese)
8. Kanari, S. : On the studies of internal waves in Lake Biwa(Ⅱ), Disaster Prevention Res. Inst. Annuals, No.12, A, pp.669-680, 1969.(in Japanese)
9. Kaneko, Y. : An example of the interfacial drag coefficient of Two-layered flows, Proc. 16th Japanese Conf. on Coastal Engineering, JSCE, pp.263-267, 1966.(in Japanese)
10. Kit, E., Berent, E. and M. Vajda : Vertical mixing induced by wind and a rotating screen in a stratified fluid in a channel, J. Hyd. Res., Vol.18, No.1, pp.35-58, 1980.
11. Muraoka, K. and T. Hirata : Internal waves in Lake Chuzenji, Proc. 27th Japanese Conf. on Hydraulics, JSCE, pp.179-184, 1983.(in Japanese)
12. Muraoka, K. and T. Hirata : Internal waves in Lake Chuzenji(Ⅱ), Proc 28th Japanese Conf. on Hydraulics, JSCE, pp.327-332, 1984.(in Japanese)
13. Nakano, S., K. Tsuruya and H. Ichinohe : Interfacial friction coefficient and entrainment coefficient in a two-layered stratified flow, Proc. 32nd Japanese Conf. on Coastal Engineering, JSCE,pp.717-721, 1985.(in Japanese)
14. Phillips, O.M. : The Dynamics of Upper Ocean, 2nd ed., Cambridge Univ. Press, pp.197, 1977.
15. Robert, J. : Internal Gravity Waves in the Ocean, Marcel Dekker, pp.97, 1975.
16. Thorpe, S.A. : On the shape of progressive internal waves, Phil. Trans. Roy. Soc. London, Ser, A, 263, pp.563-614, 1968.
17. Ura, M. : Interfacial waves and entrainment velocity across the density interface under the action of the wind stress, Proc. 30th Japanese Conf. on Coastal Engineering, JSCE, pp.561-565, 1983.(in Japanese)
18. Ura, M., T. Tsubaki and N. Matsunaga : Characteristics of flow and turbulence near the interfacial waves in upper-layer flow, J. Hydrosci. and Hydraul. Eng., JSCE, Vol.2, pp.27-45,1984.
19. Wu, J. : Wind-induced turbulent entrainment across a stable density interface, J. Fluid Mech., Vol.61, pp.275-287, 1973.

APPENDIX - NOTATION

The following symbols are used in this paper;

A_n, A_n' = factors expressing wind stress distribution, Eqs.13 and 8, respectively;

B_n, B_n' = parameters, Eq.13;

C_D = drag coefficient of wind on water surface;

F_i = $u_{s1}/\sqrt{\varepsilon g h_1}$, internal Froude number;

f, $\tilde{f}$ = interfacial friction coefficient defined by Eq.10 and its non-dimensional notation, Eq.13, respectively;

f_i = interfacial friction coefficient;

g = gravitational acceleration;

$H(t)$ = Heaviside's unit function;

h, h_1, h_2 = total depth, upper layer thickness and lower layer thickness, respectively;

k, $\tilde{k}$ = bottom friction coefficient defined by Eq.11 and its non-dimensional notation, Eq.13, respectively;

l = length of lake;

N = Brunt-Väisälä frequency;

n = integer;

n_M = Manning's roughness coefficient;

R_j = auto-correlation function;
T = fundamental period of lake;
T_a = wind stress acting on the water surface;
T_s, T_i, T_b = friction stress on water surface, interface and bottom, respectively;
U_{ma} = representative wind velocity;
U_1, U_2 = current velocities in upper and lower layers defined by Eq.9;
U_{10} = wind velocity at 10m above water surface;
u_*, U_{*n} = friction velocity of water surface due to wind stress and its amplitude, Eq.9, respectively;
u_1, u_2 = current velocities in upper and lower layers generated by internal seiche;
u_a, u_{*a} = wind velocity and friction velocity of wind on water surface;
u_r = relative velocity between upper and lower layers;
u_{s1} = mean velocity of upper layer flow;
u_{si} = interfacial velocity in wind-driven current;
x, z = coordinates taken horizontally and vertically upwards on water surface, respectively;
Z_1, Z_2 = elevations of water surface and interface defined by Eq.9, respectively;
α_1, α_2 = parameters, Eq.17;
ε = $(\rho_1 - \rho_2)/\rho_2$;
ζ_1, ζ_2 = elevations of water surface and interface caused by internal seiche;
η_1, η_2 = non-dimensional elevations of water surface and interface defined by Eq.13, respectively;
ϑ = wind intensity defined by Eq.23;
ν = kinematic viscosity of water;
ξ = x/l;
ρ, ρ_a = water density and air density;
ρ_1, ρ_2 = water density of upper and lower layers, respectively;
$\sigma_1 n$, $\sigma_2 n$ = parameters defined by Eq.17;
τ = non-dimensional time, $t/(1/\sqrt{gh})$;
υ_1, υ_2 = non-dimensional current velocity of upper and lower layers defined by Eq.13, respectively; and
Ψ = Iwasaki's number, $u_r^3/\nu\varepsilon g$.

(Received March 13, 1992; revised october 15, 1992)